[CANCER RESEARCH 64, 7732–7739, November 1, 2004]

Tid1, the Human Homologue of a *Drosophila* Tumor Suppressor, Reduces the Malignant Activity of ErbB-2 in Carcinoma Cells

Sung-Woo Kim,[1] Ta-Hsiang Chao,[1] Rong Xiang,[1] Jeng-Fan Lo,[1] Michael J. Campbell,[2] Colleen Fearns,[1] and Jiing-Dwan Lee[1]

[1]Department of Immunology, The Scripps Research Institute, La Jolla, California; and [2]Department of Surgery, University of California, San Francisco, California

ABSTRACT

The ErbB-2/HER-2 receptor tyrosine kinase is overexpressed in a wide range of solid human tumors. The ErbB-2 gene product is a transmembrane glycoprotein belonging to the epidermal growth factor receptor family, and its cytoplasmic domain is responsible for sending the mitogenic signals into cells. We discovered that this domain of ErbB-2 interacts with Tid1 protein, the human counterpart of the *Drosophila* tumor suppressor Tid56, whose null mutation causes lethal tumorigenesis during the larval stage. Tid1 also is known as a cochaperone of heat shock protein 70 (HSP70) and binds to HSP70 through its conserved DnaJ domain. We found that increased expression of Tid1 in human mammary carcinomas overexpressing ErbB-2 suppresses the expression level of ErbB-2 and attenuates the resultant ErbB-2–dependent oncogenic extracellular signal-regulated kinase 1/2 and big mitogen-activated protein kinase 1 signaling pathways leading to programmed cell death (PCD). A functional DnaJ domain of Tid1 also is required for its inhibition of ErbB-2 expression and the consequent PCD of carcinoma cells resulting from increased Tid1 expression. Importantly, ErbB-2–dependent tumor progression in animals is inhibited by increased expression of Tid1 in tumor cells. Collectively, these results suggest that Tid1 modulates the uncontrolled proliferation of ErbB-2–overexpressing carcinoma cells by reducing ErbB-2 expression and as a result suppresses the ErbB-2–dependent cancerous signaling and tumor progression. Moreover, the cochaperonic and regulatory functions of Tid1 on HSP70 most likely play an essential role in this antitumor function of Tid1 in carcinoma cells.

INTRODUCTION

ErbB-2 is a receptor tyrosine kinase that heterodimerizes with other members of the ErbB family. Its active cytoplasmic domain provides docking sites for various signaling molecules that link ErbB-2 activation to numerous intracellular signaling pathways leading to a variety of cell responses, including proliferation, differentiation, survival, and apoptosis (1, 2). Deregulation of the ErbB-2–dependent signaling network by ErbB-2 malfunction is implicated in the development of malignancy in numerous types of human cancers (3). Overexpression of ErbB-2 is found in nearly 30% of human breast and ovarian cancers and is associated with an unfavorable prognosis (4). Therefore, identifying molecules that interact with the intracellular domain of ErbB-2 will contribute not only to the elucidation of the regulatory mechanisms of ErbB-2 activity in cancer progression but also to the development of new treatments to control the growth of human cancers.

To this end, by using the cytoplasmic region of ErbB-2 as bait in a yeast two-hybrid screening, we discovered that the signaling domain of ErbB-2 interacts with Tid1 protein, which is the human counterpart of the *Drosophila* tumor suppressor Tid56 (5). Tid56 null mutation causes tumorous imaginal discs resulting from continuous cell proliferation without differentiation (5). To date, the mechanism of tumor suppression of Tid56 in *Drosophila* and the cellular function of Tid1 in human tumorigenesis are poorly understood. After confirming that Tid1 interacts with ErbB-2 in mammalian cells, we found that increasing the expression of this protein in breast cancer cells has a potent inhibitory effect on ErbB-2–dependent intracellular signaling and on the subsequent proliferation of breast cancer cells. These results suggest that Tid1 attenuates signals generated from the ErbB-2 receptor and, like its *Drosophila* counterpart, may be an important tumor suppressor, especially in breast cancer.

MATERIALS AND METHODS

Reagent and Antibodies. Unless stated otherwise, all of the other reagents were purchased from Sigma (St. Louis, MO), and all of the antibodies were purchased from Santa Cruz Biotechnology, Inc. (Santa Cruz, CA). Antiphospho–extracellular signal-regulated kinase (ERK) 1 or phosphor ErbB-2 antibodies were purchased from Upstate (Lake Placid, NY). Maria Rozakis-Adcok (McMaster University, Hamilton, ON, Canada) provided anti-Tid1 immunoblotting antibody. H5509 antibody, Tid1 COOH-terminus–specific antibody, was generated by immunizing rabbits with the KLH (Pierce, Rockford, IL)-conjugated peptide (PGTQTDQKIRMGGKGIPRINS*C*). The italicized Cys residue was added at the COOH-terminal end of each peptide for KLH conjugation reaction. M6889, Tid1 antibody described previously (6), was used for Tid1 immunoprecipitation.

Yeast Two-Hybrid Screening. The cytoplasmic tail (amino acids 676 to 1255) carrying the nucleotide binding site mutation (K753A) of human ErbB-2 cDNA was cloned into the *Nco*I and *Sal*I sites of pGBKT7 (Clontech, Palo Alto, CA) to serve as a bait vector. A human carcinoma cDNA library prepared in the pGAD-GH vector (Clontech) was used as the prey library. The mutant forms of hTid1 encoding Δ168, Δ235, ΔCT, CT, or ΔNT were fused in-frame with the GAL4-DNA activating domain of the pGAD-GH vector to define the region of hTid1 interacting with ErbB-2.

Tumor Cell Cultures. MCNeuA was derived from neu-overexpressing spontaneous mammary tumors that developed in female murine mammary tumor virus/*neu* transgenic mouse with FVB/NJ genetic background (7).

Recombinant Adenoviruses, Infections, and Transfection. A full-length cDNA encoding human Tid1 or its mutants was PCR amplified and cloned into the *Bgl*II and *Hin*dIII sites of pAdTrack-cytomegalovirus adenovirus shuttle vector (Q-BIOgene, Carlsbad, CA). Adenoviruses containing Tid1 or its mutant were used to infect breast cancer cell lines in 24-well plates (1×10^4/well) for 6 hours. Thereafter, the growth media were replaced every 2 days until completion of the experiment. Infection efficiency was checked by green fluorescence at a multiplicity of infection (1×10^7 to 3×10^7 VP). The adenovirus-infected cells were transfected with 1 μg/mL of expression plasmids encoding MEK1E or MEK5D (8) or both, using Lipofectamine 2000 (Invitrogen, Carlsbad, CA).

Apoptosis and Survival Assay. The MTT assay was used to analyze the survival of the cells. Briefly, 1×10^4 cells were seeded in each well of a 24-well plate. Ten microliters of MTT solution were added to cells and incubated at 37°C for 3 hours. The supernatant was removed, and 200 μL of DMSO were added directly to the cells. The MTT color reaction was analyzed using a microplate reader set at $A_{560\,nm}$. For apoptosis assay, apoptotic nuclear changes were detected with an *in situ* cell death detection kit, TMR red (Roche, Basel, Switzerland). The nuclei of cells were counterstained with 4′,6-diamidino-2-phenylindole staining dye (Molecular Probes Inc., Eugene, OR) for

Received 4/14/04; revised 8/20/04; accepted 8/27/04.

Grant support: Funds from National Cancer Institute (CA079871), Department of Defense BCRP (BC031105).

The costs of publication of this article were defrayed in part by the payment of page charges. This article must therefore be hereby marked *advertisement* in accordance with 18 U.S.C. Section 1734 solely to indicate this fact.

Requests for reprints: Jiing-Dwan Lee, Department of Immunology, The Scripps Research Institute, 10550 North Torrey Pines Road, La Jolla, CA 92037. E-mail: jdlee@scripps.edu.

20 minutes. For internucleosomal DNA cleavage assays, DNA preparation and agarose electrophoresis were performed as described previously (6).

Immunofluorescence. Tumor cells were plated overnight on collagen-coated glass coverslips in 12-well plates (Fisher Scientific, Hampton, NH), fixed, and permeabilized as described previously (9). After blocking in 2% normal goat serum (Vector Laboratories, Burlingame, CA) for 1 hour, the cells were incubated with antibody Neu C-18 (Santa Cruz Biotechnology, Inc.) to detect ErbB-2 or with RS-11 (Santa Cruz Biotechnology, Inc.) to detect Tid1 at 1:100 dilution for 1 hour. To amplify the Tid1 signal, the cells were incubated with biotinylated goat antimouse IgG (Vector Laboratories) for 30 minutes. The cells subsequently were incubated with Alexa Fluor 568 goat-antirabbit (red-orange) or streptavidin-conjugated–Alexa Fluor 488 antimouse antibody (green; Molecular Probes, Inc.) for 30 minutes at 1:1000 dilution. The cells were viewed and photographed with a Bio-Rad MRC1024 laser scanning confocal microscope (Hercules, CA) attached to a Zeiss Axiovert S100TV microscope (Oberkochen, Germany).

Syngenic Tumor Production. Before implantation, the tumor cells were washed twice with PBS, counted, and resuspended in PBS. MCNeuA cells (1×10^6 cells in 100 μL PBS) were inoculated subcutaneously into the right flank of FVB/NJ mice. Tumors were allowed to develop to a size of 30 mm^3. Adenovirus containing $Tid1_S$ (5×10^9 particles of virus in 100 μL PBS) were administered intratumorally at days 8, 12, and 14 after inoculation. Tumor volume (V) was calculated by: $V = (L \times W^2)/(\pi/2)$ for each tumor, where L is tumor length, and W is tumor width, and was measured at various time points as indicated after inoculation.

RESULTS

The cytoplasmic domain of ErbB-2 was used as bait in a yeast two-hybrid screen. A total of 3×10^7 transformants were screened from a human carcinoma cDNA library, and 67 positive clones were selected for sequence analysis based on their potential interaction with the intracellular part of ErbB-2. Using the BLAST algorithm and the nucleotide database at the National Library of Medicine, three clones were found to encode the COOH-terminal portion of $Tid1_S$ protein. As shown in Fig. 1*A* and *B*, the growth of transformed yeast in media lacking His and Ade is completely dependent on the presence of sequences from $Tid1_S$ and ErbB-2 in this GAL4 system. Two splicing isoforms of Tid1 exist in human cells: the long form, $Tid1_L$, and the short form, $Tid1_S$ (10). Tid1 protein contains several distinct domains: an NH_2-terminal signal sequence, a J-domain, a cysteine-rich domain resembling zinc finger repeat (CXXCXGXG), and a nonhomologous COOH-terminal domain (10). To determine which domain of Tid1 was responsible for binding to the ErbB-2 cytoplasmic domain, we tested the affinity between the signaling domain of ErbB-2 and various regions of $Tid1_S$ by yeast two-hybrid–based assays. We discovered that the COOH-terminus (amino acids 292 to 453) of $Tid1_S$ is required and sufficient for the interaction of Tid1 with ErbB-2 (Fig. 1*B*). Using the yeast expression vector encoding AD/$Tid1_L$ fusion protein in the yeast two-hybrid assay described previously, we showed that $Tid1_L$, the splicing variant of $Tid1_S$, also interacts with the signaling domain of ErbB-2 with similar affinity to that between ErbB-2 and $Tid1_S$ (Fig. 1*B*).

To further study whether ErbB-2 and Tid1 exist endogenously as a complex in mammalian cells, cell extracts from SK-BR-3 cells were immunoprecipitated with anti-Tid1 or control antibodies. The immunocomplexes were analyzed by immunoblot analysis with anti–ErbB-2 or antiphospho–ErbB-2 (pErbB-2) antibodies. As shown in Fig. 1*C*, ErbB-2 and the phosphorylated ErbB-2 copurified with Tid1. It is known that Tid1 interacts with heat shock protein 70 (HSP70) through its DnaJ domain. Therefore, it is likely that some of the cellular ErbB-2 may complex with HSP70 because of the interaction between the Tid1/ErbB-2 complex and HSP70 through the DnaJ domain of Tid1. To test this, anti-Tid1 or anti–ErbB-2 antibodies were used separately to immunoprecipitate Tid1 or ErbB-2 in the cell lysates of SK-BR-3 cells, followed by immunoblot analysis with anti-HSP70 antibody or anti-Tid1 antibody. As predicted, we found that HSP70 protein of SK-BR-3 cells exists in the immunocomplexes derived from either anti-Tid1 or anti–ErbB-2 antibodies (Fig. 1*D*). Furthermore, the short form and the long form of Tid1 were detected in the immunoprecipitates of either anti-HSP70 or anti–ErbB-2 (Fig. 1*D*). These results indicate that both forms of Tid1 interact with HSP70 and with ErbB-2.

We next investigated whether endogenous Tid1 could colocalize with the cytoplasmic domain of ErbB-2. ErbB-2 and Tid1 in SK-BR-3 cells were labeled with fluorescence by immunostaining, and their subcellular localization was visualized by confocal microscopy (Fig. 2). In SK-BR-3 cells, Tid1 is dispersed throughout the cytosol and partially colocalized with ErbB-2 (yellow, indicated with arrows, Fig. 2, *top*). This partial ErbB-2/Tid1 colocalization was blocked by overexpression of $Tid1_S$ COOH-terminal mutant (CT), which contains the

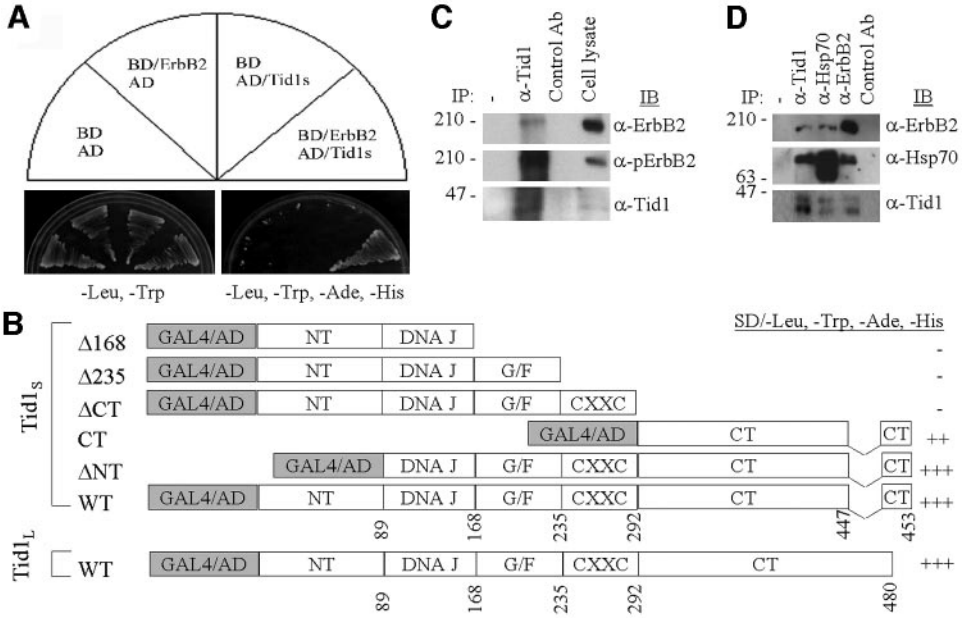

Fig. 1. Tid1 physically interacts with the signaling domain of ErbB-2. *A.,* The yeast strain PJ69–2A was cotransformed with vectors encoding a GAL4 DNA binding domain (*BD*) fusion protein (BD/cytoplasmic domain of ErbB-2) along with the indicated GAL4 active domain (*AD*) fusion protein. Transformed yeast was cultured on plates containing the indicated selective media. *B.* The COOH-terminus of $Tid1_S$ is required for interaction with ErbB-2. Schematic representations of Tid1 protein and its deletion derivatives used as bait in the yeast two-hybrid screen. The presence (+) and absence (−) of interaction between Tid1 mutants and ErbB-2 is shown. *C.* Lysates from SK-BR-3 were immunoprecipitated with either M6689, an anti-Tid1 antibody (6), or control antibodies as indicated. Immunocomplexes were electroblotted onto nitrocellulose filters, and coprecipitated ErbB-2, pErbB-2, or precipitated Tid1 was detected with anti–ErbB-2, anti–pErbB-2, or anti-Tid1 antibodies separately. In total cell lysates, the presence of endogenous Tid1 and ErbB-2 proteins was detected with either anti-Tid1 or anti–ErbB-2 antibodies (last lane of each panel). *D.* The immunoprecipitated samples from SK-BR-3 cells using anti-Tid1, anti–ErbB-2, anti-HSP70, or control antibodies were immunoblotted with anti-HSP70 or anti-Tid1 antibodies.

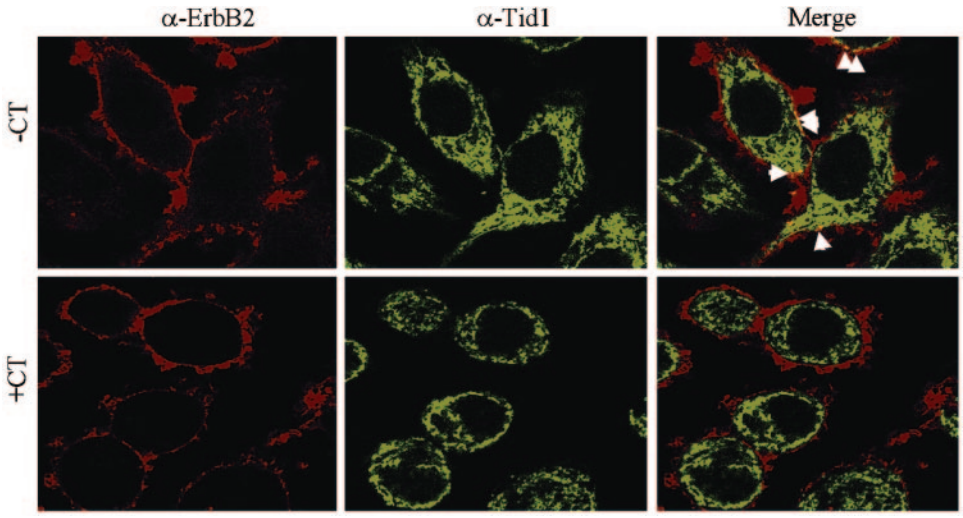

Fig. 2. Colocalization of ErbB-2 and Tid1 in mammary carcinoma cells. SK-BR-3 cells were infected with (*bottom*) or without (*top*) COOH-terminal mutant form of Ad-Tid1$_S$ and were immunostained with anti–ErbB-2 and anti-Tid1 antibodies to detect the colocalization of ErbB-2 (*left, red fluorescence*) and Tid1$_S$ (*middle, green fluorescence*). The merge of red and green fluorescence is shown in the right panels (*yellow*). Colocalization is indicated with arrows.

domain of Tid1 that interacts with ErbB-2 (Fig. 2, *bottom*). The colocalization of ErbB-2 with hTid1$_S$ appears to occur near the inner plasma membrane, where the ErbB-2 cytoplasmic tail most likely is located. As expected, in previous reports it was shown that Tid1 is distributed in the cytoplasm and the nucleus because it interacts with several cellular proteins (10–12). Moreover, in *Drosophila*, Tid56 was reported to interact with the Hedgehog-bound Patched receptor (13). Our data of the interaction between Tid1 and ErbB-2 and the colocalization of Tid1 and ErbB-2 further support the notion that Tid1 interacts with membrane-bound receptors not only in insect cells but also in mammalian cells.

To assess the function of Tid1 in human breast cancer cell lines, breast carcinoma cells with high expression levels (SK-BR-3 and BT-474) or with low expression levels (MDA-MB-231) of ErbB-2 were tested (Fig. 3*A*). Cells were infected with recombinant adenovirus encoding either Tid1$_S$ or Tid1$_L$ resulting in increased levels of Tid1$_S$ or Tid1$_L$, respectively (Fig. 3*B*). Proliferation of ErbB-2–overexpressing cells infected with Ad-Tid1$_S$ was inhibited after 48 hours, and the number of viable cells later gradually decreased, most likely because of cell death (Fig. 3*C*). Increased expression of Tid1$_L$ had a similar effect to that of Tid1$_S$ in these cell lines (Fig. 3*C*). Interestingly, the growth-inhibitory effect of overexpression of Tid1$_L$ or Tid1$_S$ was not observed in MDA-MB231 cells, which express only low levels of ErbB-2. These data indicate that increased Tid1 expression blocks the proliferation of human carcinomas that overexpress ErbB-2.

To ascertain whether the growth inhibitory and cell death effect of Tid1$_S$ in ErbB-2–overexpressing cells is caused by apoptosis and to locate a domain(s) of Tid1$_S$ responsible for the cell death, we generated recombinant adenovirus encoding wild-type or mutant derivatives of Tid1$_S$ proteins (Fig. 4*A*). SK-BR-3 cells were infected with these viruses and checked for expression of the wild-type or mutant Tid1 proteins (Fig. 4*B, top*). Typical apoptotic morphology characterized by loss of adherence, condensed cytoplasm, and formation of

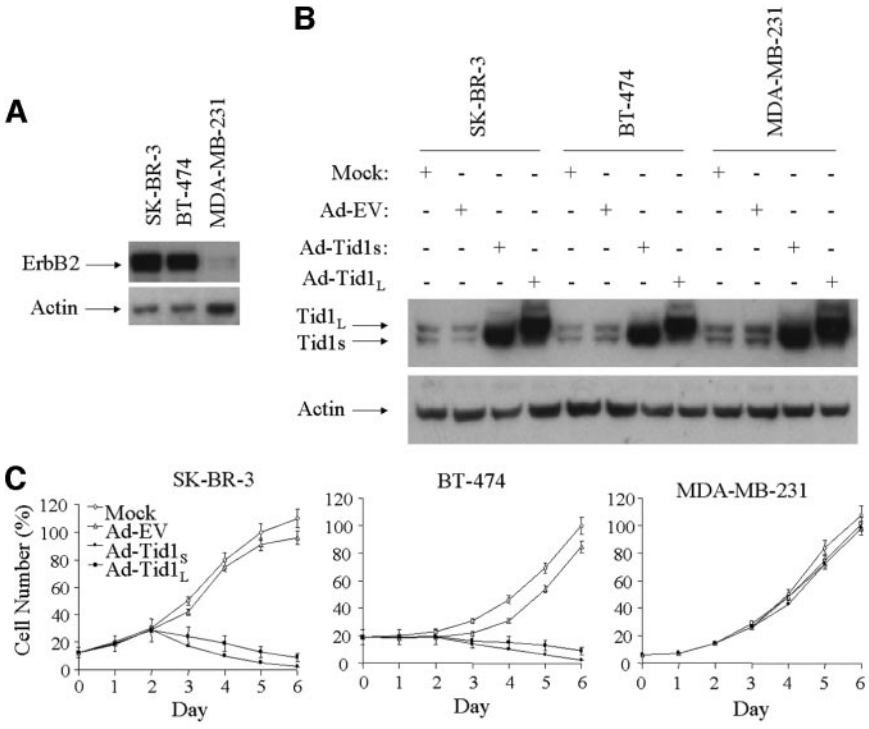

Fig. 3. Increased cellular Tid1 induces growth arrest and cell death in ErbB-2–overexpressing breast cancer cells. *A.* The levels of ErbB-2 expression were detected in the cell lysates of SK-BR-3, BT-474, and MDA-MB-231 with an anti–ErbB-2 antibody in an immunoblot assay. *B,* overexpression of Tid1$_L$ or Tid1$_S$ in various cancer cell lines. Cells were mock infected or were infected with empty virus (Ad-EV) or with viruses encoding either Tid1 short form (Ad-Tid1$_S$) or long form (Ad-Tid1$_L$) as indicated. Two days after infection, levels of Tid1 were analyzed by immunoblot analysis. *C.* SK-BR-3, BT-474, and MDA-MB-231 cells were treated as in *B*. The growth of these cells was analyzed by MTT assay at the indicated day after infection. The MTT value of the day 6 mock-infected cells was taken as 100%.

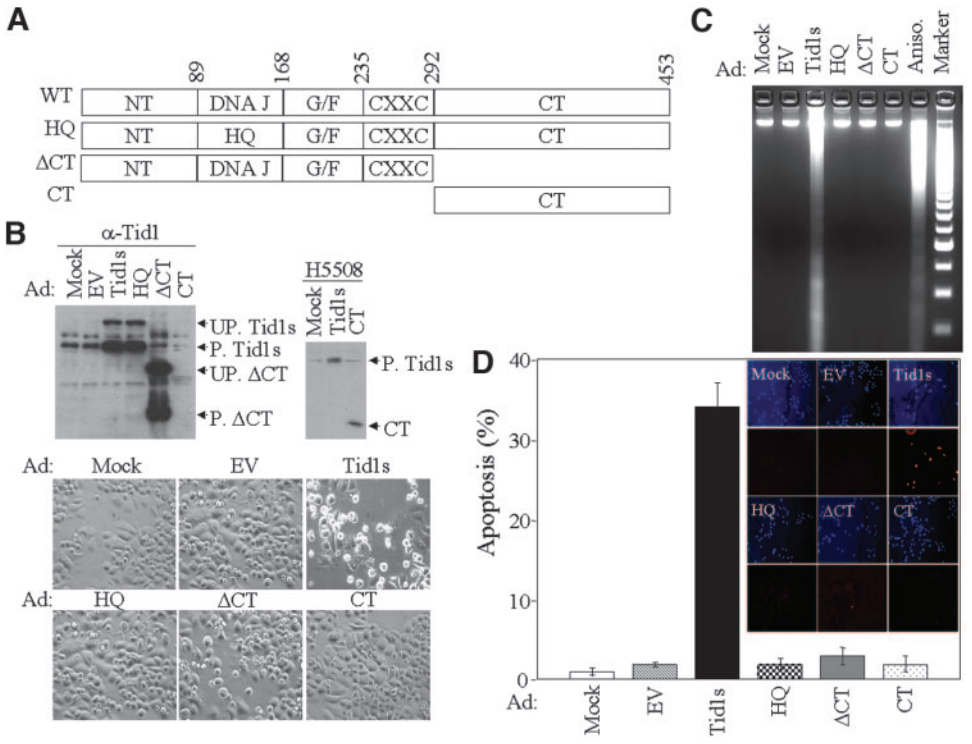

Fig. 4. Increased cellular Tid1 leads to apoptosis of cancer cells. *A,* diagram of Tid1 deletion mutant constructs. *B,* SK-BR-3 cells were mock infected (*Lane 1*) or infected with Ad-EV (*Lane 2*), Ad-Tid1$_S$ (*Lane 3*), or its mutants as indicated (*Lanes 4* to *6*). Cell extracts from these cells were analyzed by immunoblot analysis using anti-Tid1 antibody (*top left*). Because this anti-Tid1 antibody is not able to detect the COOH-terminal of Tid1$_S$, H5509, an antibody that specifically detects the COOH-terminus of Tid1, was used for detecting the expression of Tid1$_S$-CT mutant (*top right*). The arrows indicate the processed form (*P*) or the unprocessed form (*UP*) of Tid1$_S$ and its mutants. *Bottom,* phase contrast images of cells 6 days after infection with the indicated viruses. *C,* SK-BR-3 cells were infected as in *B*. Seventy-two hours after infection, genomic DNA from these cells was prepared and analyzed for DNA laddering. As a positive control for DNA laddering, cells were treated with 5 μg of anisomycin/mL for 18 hours. *D,* SK-BR-3 cells were treated with viruses as in *B*. Six days after infection, these cells were stained with 4′,6-diamidino-2-phenylindole (blue) and the *in situ* TUNEL assay (*red*; Cell Death Detection Kit, TMR red); *% apoptosis*, red cell number per total cell number.

apoptotic bodies in dying cells was observed by light microscopy 6 days postinfection with Ad-Tid1$_S$ (Fig. 4*B, bottom*). Similar results also were found in the cells infected with Ad-Tid1$_L$, indicating Tid1$_L$ has a similar apoptosis-inducing effect on carcinoma cells as Tid1$_S$ (data not shown). The appearance of a DNA ladder indicative of typical apoptosis was detected in samples prepared from cells infected with Ad-Tid1$_S$ 3 days after infection (Fig. 4*C*). In contrast, no apoptosis or DNA laddering was observed in cells infected with the Ad-Tid1$_S$ mutants (Fig. 4*B, bottom* and *C*). The percentage of cells undergoing programmed cell death (PCD) was quantified by terminal deoxynucleotidyl transferase-mediated nick end labeling (TUNEL) assay (Fig. 4*D*). Approximately 35% of the ErbB-2–overexpressing cells with increased expression of Tid1$_S$ were apoptotic, whereas apoptotic bodies were found in only 1% to 3% of those cells infected with control adenovirus or adenoviruses encoding mutant Tid1$_S$. Interestingly, none of the Tid1$_S$ mutants, including the J domain mutant (HQ), COOH-terminal deletion mutant (ΔCT), and CT mutants (Fig. 4*A*), induced apoptosis. These data suggest that the DnaJ domain (critical for the binding of Tid1 to HSP70) and the COOH-terminus of Tid1 (responsible for its interaction with ErbB-2; Fig. 1*B*) are required for Tid1-mediated apoptosis. Furthermore, active caspase-3 increased significantly in the cells infected with Ad-Tid1$_S$ compared with those cells uninfected (mock) or infected with control virus (Ad-EV), confirming that the apoptosis induced by increased intracellular Tid1 is concomitant with the production of active caspase-3 (Fig. 5*A*). Treatment with z-Val-Ala-Asp, a caspase-3 inhibitor, also was able to attenuate cell death induced by increased expression of Tid1 in SK-BR-3 cells (Fig. 5*B*), indicating that caspase-3 is involved in this Tid1-induced apoptosis. To further examine the contribution of each domain of Tid1 in Tid1-mediated cell death, we tested whether apoptosis induced by increased Tid1 can be influenced by intracellular expression of Tid1 mutants. Ad-Tid1$_S$–

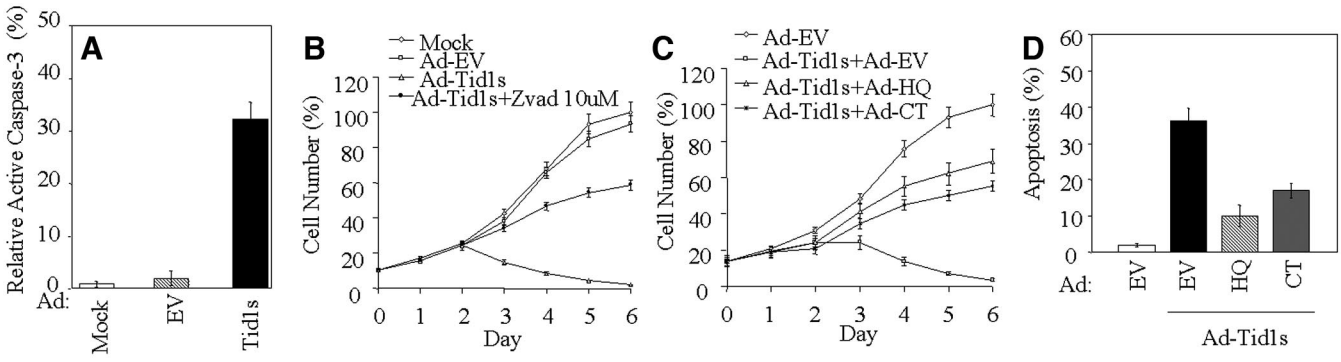

Fig. 5. The DnaJ and COOH-terminal domains of Tid1 are critical for the Tid1-mediated PCD in breast cancer cells overexpressing ErbB-2. *A,* SK-BR-3 cells were mock infected or infected with control virus (Ad-EV) or Ad-Tid1$_S$ as indicated. Three days later, these cells were fixed and stained with 4′,6-diamidino-2-phenylindole (*blue, top*) and antiactive caspase-3 antibody (*red, bottom*). Red cells were counted as active caspase-3–positive cells; *% active caspase-3 cell*, red cell number per total cell number. *B,* SK-BR-3 cells were treated with viruses as in *A*, followed by incubation with or without the caspase inhibitor (z-Val-Ala-Asp, 25 imol/L). The growth of these treated cells was assessed by MTT assay at the indicated days after infection. The MTT value of control virus–infected cells at day 6 was taken as 100%. *C.* Ad-Tid1$_S$–infected SK-BR-3 cells were coinfected with Ad-EV or Ad-Tid1$_S$ mutants (HQ or CT) as indicated. The growth of these cells was analyzed by MTT assay at the indicated times after infection. The MTT value of day 6 control virus–infected cells was taken as 100%. *D,* SK-BR-3 cells were treated as in *C*. Three days later, the apoptosis of these cells was measured using TUNEL assay; *% apoptosis*, red cell number per total cell number. Results are expressed as the mean ± SE.

infected SK-BR-3 cells were coinfected with individual Ad-Tid1$_S$ mutants. Overexpression of Tid1 with a mutated J domain (HQ) or a Tid1 deletion mutant only expressing COOH-terminal of Tid1 (CT) blocked the apoptosis of Ad-Tid1$_S$–infected SK-BR-3 cells (Fig. 5*C* and *D*). Collectively, these results suggest that increased Tid1 in ErbB-2–overexpressing cells leads to apoptosis, and the Tid1 domains required for ErbB-2 interaction (COOH-terminal) and HSP70 binding (J domain) are critical in this Tid1-mediated PCD of cancer cells.

We next investigated the activity and the protein level of ErbB-2 in SK-BR-3 cells infected with Ad-Tid1$_S$ and found that these cells, compared with cells treated with control virus, had significantly less ErbB-2 and phospho–ErbB-2 proteins but had similar amounts of actin (Fig. 6*A*). Because HSP70 may be involved in regulating ErbB-2 stability by ubiquitination-mediated degradation and because Tid1 is a cochaperone of HSP70 (14, 15), we wondered whether Tid1 has a role in destabilizing ErbB-2 protein by enhancing ErbB-2 ubiquitination. As shown in Fig. 6*B*, increased expression of Tid1$_S$ significantly promoted the ubiquitination of ErbB-2, as revealed by antiubiquitin immunoblot analysis in immunoprecipitates of ErbB-2 from cells infected with Ad-Tid1$_S$ (Fig. 6*B, left*, compare *Lane 3* with *Lanes 1* and *2*). Because ubiquitinated proteins are highly unstable and are quickly degraded by proteasomes, the proteasome inhibitor MG-132 was added to the cells 4 hours before lysing the cells to facilitate the observation of the Tid1-dependent ErbB-2 ubiquitination (Fig. 6*B, right,* compare *Lane 3* with *Lanes 1* and *2*). Because Tid1-CT mutant binds to ErbB-2 signaling domain and thus may serve as a dominant negative by inhibiting the binding of Tid1 to ErbB-2, it also was interesting to test whether the down-regulation of ErbB-2 could be blocked by overexpression of Tid1-CT in SK-BR-3 cells treated with Ad-Tid1$_S$. The ErbB-2 down-regulation in Ad-Tid1$_S$–treated SK-BR3 cells was reversed by coinfecting these cells with Ad-Tid1-CT (Fig. 6*C*). We also observed some increase in ErbB-2 expression in SK-BR3 cells infected with Ad-Tid1-CT alone, which might have resulted from inhibition of endogenous Tid1-mediated down-regulation of ErbB-2 (Fig. 6*C*). Collectively, these data suggest that Tid1 induces ErbB-2 down-regulation via the ubiquitin pathway.

Tyrosine phosphorylation of specific cytoplasmic residues of ErbB-2 recruits binding of signaling molecules, including adaptor molecules that allow activation of specific intracellular oncogenic pathways (2, 3, 16, 17). Among them, mitogen-activated protein kinase (MAPK) pathways and the phosphatidylinositol 3′-kinase/AKT pathway are known to supply proliferative and survival signals, and these pathways have been shown to be critical for the malignant properties of ErbB-2–dependent carcinomas (2, 17, 18). Thus, we investigated whether the activities of these pathways were affected by ErbB-2 protein reduction in Ad-Tid1$_S$–infected SK-BR-3 cells. Phosphorylation of MAPKs, ERK1/2, and big mitogen-activated protein kinase 1 (BMK1)/ERK5 was substantially attenuated in the cells treated with Ad-Tid1$_S$ (Fig. 6*D*). In contrast, there was no difference in AKT phosphorylation between cells infected with Ad-Tid1$_S$ and with control viruses. These results indicated that MAPK pathways, ERK1/2, and BMK1 cascades are the major targeted signaling pathways during Tid1-dependent ErbB-2 deactivation. We next examined the contribution of each of these attenuated MAPK pathways to Ad-Tid1$_S$–induced PCD of carcinoma cells by selectively activating these pathways individually or jointly using MEK1E, the dominant active form of MEK1 (for the ERK1/2 pathway), and/or MEK5D, the dominant active form of MEK5 (for the BMK1 pathway) in Ad-Tid1$_S$–infected SK-BR-3 cells (Fig. 7*A*). We found that the expression of MEK1E or MEK5D up-regulated the activity of ERK1/2 or BMK1, respectively, and partially inhibited the PCD of SK-BR-3 induced by increased Tid1 expression (Fig. 7*B* and *C*). Cotransfection of MEK1E and MEK5D into Ad-Tid1$_S$–infected SK-BR-3 cells had an additive effect in rescuing these cells from apoptosis (Fig. 7*B* and *C*), indicating that although the activity of ERK1/2 and BMK1 pathways is critical for sustaining SK-BR-3 cell growth and survival, there is little overlap between these two pathways in delivering the survival signals from ErbB-2 for SK-BR-3 cells.

We next tested whether increased Tid1 expression inhibited the development of ErbB-2–dependent tumors in animals. A mouse ErbB-2–dependent mammary carcinoma cell line (McNeuA) was

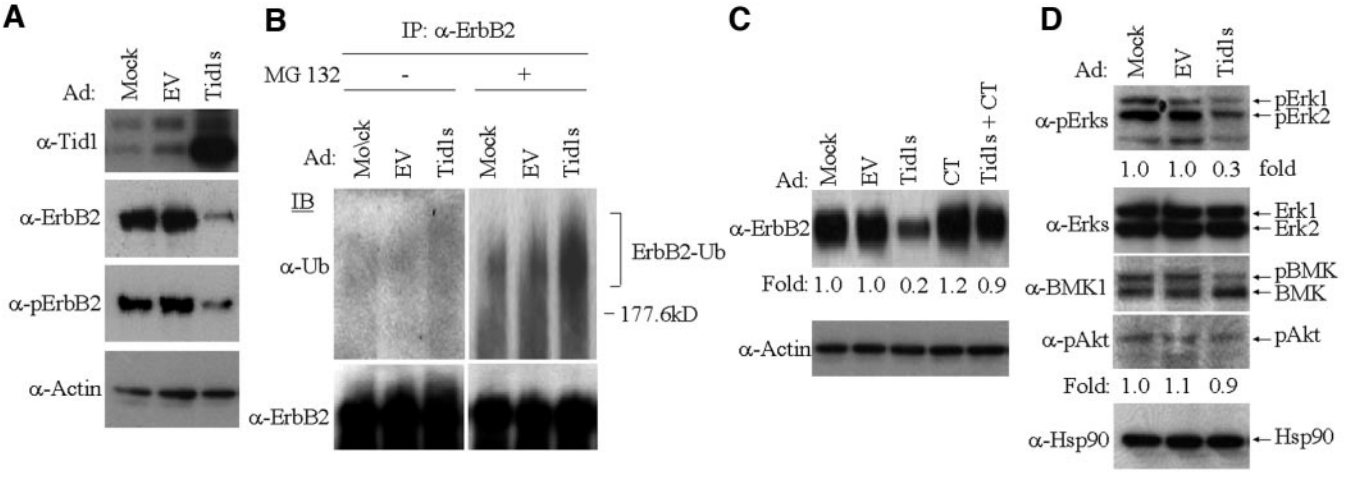

Fig. 6. Tid1$_S$ negatively regulates ErbB-2 signaling pathways by enhancing the degradation of ErbB-2. *A.* SK-BR-3 cells were mock infected or were infected with Ad-EV or Ad-Tid1$_S$ as indicated and were lysed after 2 days. Cell lysates were immunoblotted with the indicated antibodies. *B.* Cells infected with control viruses or Ad-Tid1$_S$ as indicated were treated with (*right*) or without (*left*) 50 μmol/L proteasome inhibitor MG-132 for 4 hours before lysis. The total cell lysates were immunoprecipitated with anti–ErbB-2 antibody, followed by SDS-PAGE and immunoblot with either antiubiquitin (*α-Ub*; *top*) or anti–ErbB-2 antibodies (*bottom*). *C.* SK-BR-3 cells were mock infected (*Lane 1*) or infected with Ad-EV (*Lane 2*), Ad-Tid1$_S$ (*Lane 3*), Ad-Tid1$_S$-CT (*Lane 4*), or with the combination of Ad-Tid1$_S$ and Ad-Tid1$_S$-CT (*Lane 5*) as indicated. Two days later, cell extracts from these infected cells were analyzed by immunoblot analysis with anti–ErbB-2 antibody (*top*) or antiactin antibody (*bottom*). *D.* The same total cell lysates from *B*, without MG-132 treatment, were analyzed by SDS-PAGE, followed by immunoblot anaylsis with anti-pERK1/2, anti-ERK1/2, anti-BMK1, anti-pAkt, or anti-HSP90 antibodies as indicated. Fold of activation of ERK1/2 or Akt was estimated by scanning the immunoblots of the first or third panel using a densitometer. The intensity of band derived from mock-infected cells was taken as one.

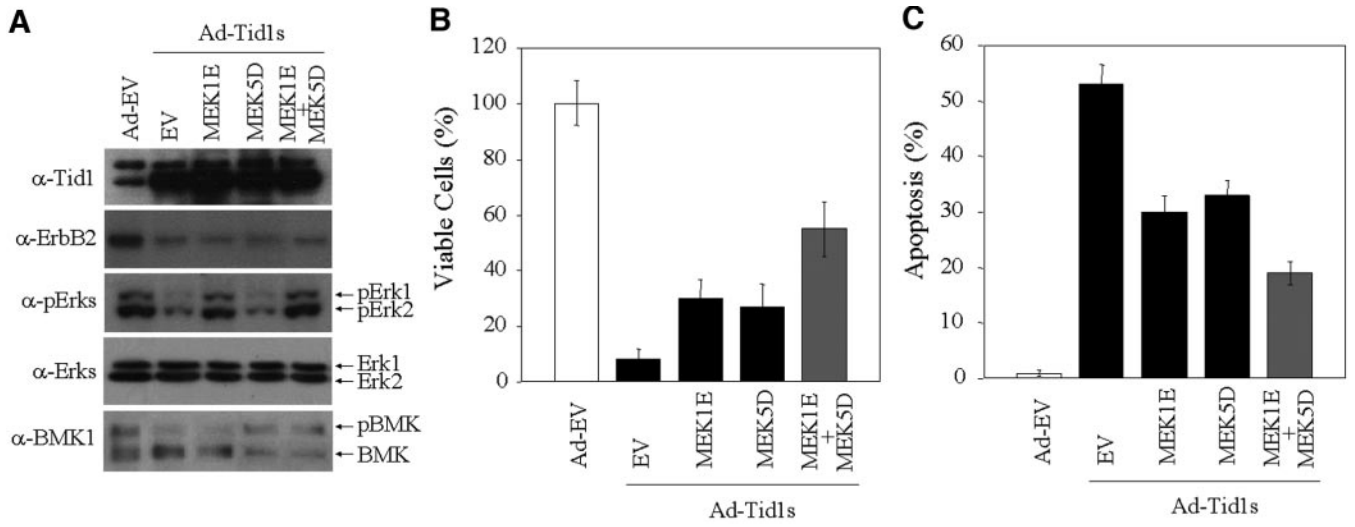

Fig. 7. Down-regulation of ERK1/2 and BMK1 MAPK pathways contributes to the Tid1-mediated PCD of mammary cancer cells overexpressing ErbB-2. *A.* SK-BR-3 cells were incubated with Ad-Tid1$_S$ for 6 hours, and the medium then was replaced with fresh medium. The cells then were transfected with expression plasmids encoding MEK1E and/or MEK5D as indicated. Cell lysates were prepared 2 days after transfection and immunoblotted with the indicated antibodies. *B.* SK-BR-3 cells were infected and later transfected as in *A*. Four days after transfection, the number of viable cells was assessed by MTT assay. The MTT value of Ad-EV–infected cells was taken as 100%. *C,* SK-BR-3 cells were treated as in *A*. Three days after transfection, apoptosis of these cells was measured using TUNEL assay; *% apoptosis,* red cell number per total cell number. Results are expressed as the mean ± SE.

infected with Ad-Tid1$_S$ (Fig. 8*A*), and these treated cells stopped proliferating and started to die 3 days after infection (Fig. 8*B*), similar to what we observed in SK-BR-3 and BT-474 cells. Because murine syngeneic models of this mammary carcinoma are available (7), we investigated whether increased expression of Tid1$_S$ would inhibit the growth of ErbB-2–dependent tumors in mice. McNeuA cells first were infected with Ad-EV or Ad-Tid1$_S$ and then subcutaneously inoculated into FVB/NJ syngeneic mice. Whereas all of the mice injected with noninfected cells or cells infected with Ad-EV developed tumors, none of the mice injected with Ad-Tid1$_S$–infected cells showed progressive tumor growth during the observation period (Fig. 8*C*). To investigate whether administration of Ad-Tid1$_S$ intratumorally would attenuate the growth of pre-existing ErbB-2–dependent tumors, McNeuA cells first were inoculated subcutaneously into the right flank of FVB/NJ syngenic mice. After the tumors developed to ~30 mm^3, the tumor-bearing mice were administered intratumorally with vehicle, control virus, or Ad-Tid1$_S$ on days 8, 12, and 14. The treatment of Ad-Tid1$_S$ induced a significant reduction in tumor volumes: ~70% reduction compared with treatment with vehicle or ~50% reduction compared with Ad-EV (Fig. 8*D*). Collectively, these results suggest that increased expression of Tid1 has an antitumor effect on the development of ErbB-2–dependent carcinomas in animals.

DISCUSSION

Overexpression of the transmembrane receptor tyrosine kinase ErbB-2 is frequent in mammary and ovarian tumors and is indicative of an unfavorable clinical prognosis. Thus, ErbB-2 is known as a molecular target for therapy through reduction of ErbB-2 signaling. One physiologic mechanism to reduce oncogenic signaling of the ErbB family of growth factor receptors is through down-regulation of their expression on the cell surface by ligand-induced endocytosis, followed by lysosome-mediated degradation. Intracellular Cbl proteins interact with ErbB-1 during this process, thereby facilitating its ubiquitination and subsequent degradation (19). However, ErbB-2 fails to bind Cbl and thus avoids ubiquitination and degradation mediated by Cbl proteins. Other ErbB family members that heterodimerize with ErbB-2 also can escape the Cbl-dependent lysosomal degradation, resulting in enhanced

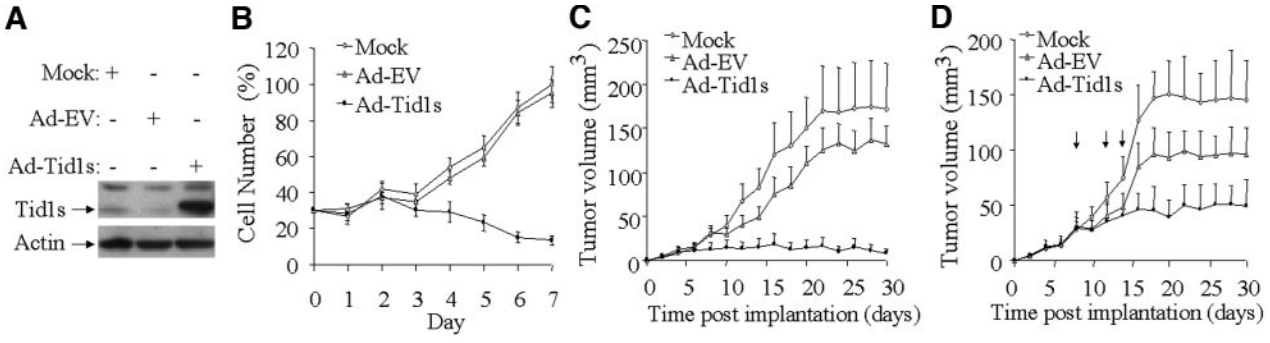

Fig. 8. Increased cellular Tid1 inhibits the growth of ErbB-2–dependent tumors in animals. *A,* increased expression of Tid1$_S$ in McNeuA cells infected with Ad-Tid1$_S$. McNeuA cells were mock infected or infected with Ad-EV or Ad-Tid1$_S$. Two days later, the cells were lysed and analyzed by immunoblot analysis using anti-Tid1 or antiactin antibodies as indicated. *B,* McNeuA cells were mock infected or infected with Ad-EV or Ad-Tid1$_S$. The growth of these cells was examined by MTT assay at the indicated times after infection. The MTT value of mock-infected cells was taken as 100%. *C,* McNeuA cells were treated as in *A*. Two days after treatment, these cells (1×10^6 cells) were inoculated subcutaneously into the right flank of FVB/NJ mice (five mice per group). Tumor volumes were measured at the indicated day after injection. *D,* McNeuA cells (1×10^6 cells) were subcutaneously inoculated into FVB/NJ mice and later allowed to develop tumors to a size of ~30 mm^3 (8 days). These tumor-bearing mice then were randomized into three treatment groups (six mice per group). On days 8, 12, and 14 after implantation, progressively growing McNeuA tumors were treated with intratumoral injections of Ad-Tid1$_S$, Ad-EV, or PBS (vehicle) as indicated. Tumor volumes were measured at the indicated day after initial McNeuA cell injection. Results are expressed as the mean ± SE.

mitogenic signaling. Herein, we found that intracellular Tid1 protein interacts with the signaling domain of ErbB-2 and promotes the ubiquitination and degradation for ErbB-2, leading to subsequent attenuation of the oncogenic signaling from ErbB-2 in carcinoma cells. It has been shown that one mechanism of ErbB-2 ubiquitination and degradation is mediated by an HSP70-dependent pathway in which carboxyl terminus HSP70-interacting protein (CHIP) serves as an ubiquitin ligase (14, 20). However, the mechanism by which ErbB-2 is brought to the HSP70/CHIP complex is poorly understood. Our finding of the interaction of ErbB-2 with Tid1, an HSP70 cochaperone protein, and the subsequent enhancement of ErbB-2 ubiquitination suggests that Tid1 may participate in ErbB-2 degradation mediated by the HSP70/CHIP complex by facilitating the association of ErbB-2 with HSP70 chaperones. Tid1 also contains a cysteine-rich domain, which may serve as a RING finger domain critical for the function of ubiquitin ligases (21). However, whether Tid1 is directly involved in ubiquitination of ErbB-2 is not clear and needs additional investigation.

As shown in Fig. 6*D*, we observed no change in AKT activity after down-regulation of ErbB-2 level by increased expression of Tid1 in SK-Br-3 cells. This is in contrast to several reports that have described a decrease in AKT activity after reduction of ErbB-2 levels in cancer cells (2, 22). In these reports, down-regulation of ErbB-2 was achieved by treatment with Herceptin, ErbB-2–specific antisense oligonucleotides, or ansamycin antibiotics. These treatments, except for ansamycin, are specific for ErbB-2. In our system, however, down-regulation is achieved through Tid1, and Tid1 has been reported to modulate various oncogenic signaling pathways other than ErbB-2, such as Ras, Janus-activated kinase/signal transducers and activators of transcription, and nuclear factor κB pathways (11, 18, 23). Thus, it may be that activation of these pathways by Tid1 compensates for the reduction in oncogenic signals derived from ErbB-2 itself. To this end, AKT has been shown to be either a downstream or an upstream regulator of nuclear factor κB (24). Thus, we suspect that increased expression of Tid1 in SK-Br-3 cells may influence AKT activity indirectly through its regulation of signaling pathway(s), such as nuclear factor κB.

Tid1 is the only human homologue of the *Drosophila* tumor suppressor gene Tid56. Tid56 null mutation causes tumorous imaginal discs resulting from continuous cell proliferation without differentiation (5, 13). To date, the mechanism of tumor suppression of Tid56 in *Drosophila* and the cellular function of Tid1 in human tumorigenesis are poorly understood. In light of our finding that human Tid1 attenuates ErbB-2 activity and blocks the proliferation of ErbB-2–overexpressing cells, it is possible that Tid56 regulates the activity of an epidermal growth factor receptor (EGFR) homologue in *Drosophila*. In the *Drosophila* genome, there is only one member of the EGFR family, DER, which is highly expressed in imaginal discs and has an instructive role in the proliferation and differentiation of these discs (25). DER activity is tightly regulated in time and space by positive and negative regulators to ensure the precise development of the discs. It is likely that the antitumor function of Tid56 results from, at least in part, its ability to negatively regulate DER activity during larval life. Additionally, in Fig. 8, we have shown that Ad-Tid1$_S$ treatment of ErbB-2–dependent tumors resulted in significant reduction in tumor volumes in a syngeneic tumor model. Although there are technical drawbacks to using adenoviruses, such as variations in infectivity of cultured tumor cell lines and variable nonspecific cytotoxic effects, these studies showed that Ad-Tid1$_S$ has significant therapeutic implications for mammalian tumors.

Tid1 also has been shown to regulate the activity of other mitogenic or oncogenic intracellular proteins, such as human papillomavirus E7 oncoprotein, RasGAP, Jak2 kinase, and HTLV-1 Tax protein (11, 18, 23, 26). Most of these molecules are known to be carcinogenic in various human tissues. It is possible that, in addition to ErbB-2, Tid1 also exerts its antitumor function through modulating the activities of these signaling pathways. Most recently, it has been shown that reduction of physiologic levels of Tid1 in cancer cell lines resulted in higher resistance to apoptosis induced by multiple exogenous stimuli, including tumor necrosis factor α (27), suggesting that Tid1 could exercise its tumor suppressor activity by playing a role as a cell death regulator in mammalian cells. Therefore, the potential anticancer activity of Tid1 in animals may affect multiple oncogenic pathways. To clearly determine the function of Tid1 in tumor development, it is critical to establish an animal model in which the expression of Tid1 in various cancer prone tissues can be modulated. The global deletion of Tid1 leads to early embryonic lethality in Tid1-null mice, preventing us from investigating the role of Tid1 in tumorigenesis in adult animals (6). Thus, we have generated a conditional knockout mouse model for the *Tid1* gene to circumvent the issue of early death in Tid1-null mice. We currently are deleting the *Tid1* gene in selective tissues (*e.g.,* mammary epithelium) of these mice by crossing them with transgenic mice carrying tissue-specific expressed *Cre* genes to evaluate the contribution of Tid1 toward various aspects of malignancies in different tissues of mammals.

REFERENCES

1. Olayioye MA, Neve RM. Lane HA, Hynes NE. The ErbB signaling network: receptor heterodimerization in development and cancer. EMBO J 2000;19:3159–67.
2. Basso AD, Solit DB. Munster PN, Rosen N. Ansamycin antibiotics inhibit Akt activation and cyclin D expression in breast cancer cells that overexpress HER2. Oncogene 2002;21:1159–66.
3. Zhou BP, Hung MC. Dysregulation of cellular signaling by HER2/neu in breast cancer. Semin Oncol 2003;30:38–48.
4. Hayes DF, Thor AD. c-erbB-2 in breast cancer: development of a clinically useful marker. Semin Oncol 2002;29:231–45.
5. Kurzik-Dumke U, Gundacker D, RenthropM, Gateff E. Tumor suppression in Drosophila is causally related to the function of the lethal(2) tumorous imaginal discs gene, a dnaJ homolog. Dev Genet 1995;16:64–76.
6. Lo JF, Hayashi M, Woo-Kim S, et al. Tid1, a cochaperone of the heat shock 70 protein and the mammalian counterpart of the Drosophila tumor suppressor l(2)tid, is critical for early embryonic development and cell survival. Mol Cell Biol 2004;24:2226–36.
7. Campbell MJ, Wollish WS, Lobo M, Esserman LJ. Epithelial and fibroblast cell lines derived from a spontaneous mammary carcinoma in a MMTV/neu transgenic mouse. In Vitro Cell Dev Biol Anim 2002;38:326–33.
8. Kato Y, Kravchenko VV, Tapping RI, Han J, Ulevitch RJ, Lee JD. BMK1/ERK5 regulates serum-induced early gene expression through transcription factor MEF2C. EMBO J 1997;16:7054–66.
9. Kim SW, Hayashi M, Lo JF, Yang Y, Yoo JS, Lee JD. ADP-ribosylation factor 4 small GTPase mediates epidermal growth factor receptor-dependent phospholipase D2 activation. J Biol Chem 2003;278:2661–8.
10. Syken J, De Medina T, Munger K. TID1, a human homolog of the Drosophila tumor suppressor l(2)tid, encodes two mitochondrial modulators of apoptosis with opposing functions. Proc Natl Acad Sci USA 1999;96:8499–504.
11. Trentin GA, Yin X, Tahir S, et al. A mouse homologue of the Drosophila tumor suppressor l(2)tid gene defines a novel Ras GTPase-activating protein (RasGAP)-binding protein. J Biol Chem 2001;276:13087–95.
12. Cheng H, Cenciarelli C, Shao ZP, et al. Human T cell leukemia virus type 1 Tax associates with a molecular chaperone complex containing hTid-1 and Hsp70. Curr Biol 2001;11:1771–5.
13. Canamasas I, Debes A, Natali PG, Kurzik-Dumke U. Understanding human cancer using Drosophila–Tid47, a cytosolic product of the DnaJ-like tumor suppressor gene l(2)tid, is a novel molecular partner of patched related to skin cancer. J Biol Chem 2003;278:30952–60.
14. Xu W, Marcu M, Yuan X, Mimnaugh E, Patterson C, Neckers L. Chaperone-dependent E3 ubiquitin ligase CHIP mediates a degradative pathway for c-ErbB2/Neu. Proc Natl Acad Sci USA 2002;99:12847–52.
15. Jiang JH, Ballinger CA, Wu YX, et al. CHIP is a U-box-dependent E3 ubiquitin ligase—identification of Hsc70 as a target for ubiquitylation. J Biol Chem 2001;276:42938–44.
16. Calabrese C, Frank A, Maclean K, Gilbertson R. Medulloblastoma sensitivity to 17-allylamino-17-demethoxygeldanamycin requires MEK/ERK. J Biol Chem 2003;278:24951–9.

17. Esparis-Ogando A, Diaz-Rodriguez E, Montero JC, Yuste L, Crespo P, Pandiella A. Erk5 participates in neuregulin signal transduction and is constitutively active in breast cancer cells overexpressing ErbB2. Mol Cell Biol 2002;22:270–85.
18. Cheng H, Cenciarelli C, Tao MY, Parks WP, Cheng-Mayer C. HTLV-1 tax-associated hTid-1, a human DnaJ protein, is a repressor of I κ B kinase ā subunit. J Biol Chem 2002;277:20605–10.
19. Levkowitz G, Klapper LN, Tzahar E, Freywald A, Sela M, Yarden Y. Coupling of the c-Cbl protooncogene product to ErbB-1/EGF-receptor but not to other ErbB proteins. Oncogene 1996;12:1117–25.
20. Zhou P, Fernandes N, Dodge IL, et al. ErbB2 degradation mediated by the co-chaperone protein CHIP. J Biol Chem 2003;278:13829–37.
21. Maloney A, Workman P. HSP90 as a new therapeutic target for cancer therapy: the story unfolds. Expert Opin Biol Ther 2002;2:3–24.
22. Cuello M, Ettenberg SA, Clark AS, et al. Down-regulation of the erbB-2 receptor by trastuzumab (herceptin) enhances tumor necrosis factor-related apoptosis-inducing ligand-mediated apoptosis in breast and ovarian cancer cell lines that overexpress erbB-2. Cancer Res 2001;61:4892–900.
23. Sarkar S, Pollack BP, Lin KT, et al. hTid-1, a human DnaJ protein, modulates the interferon signaling pathway. J Biol Chem 2001;276:49034–42.
24. Meng F, Liu L, Chin PC, D'Mello SR. Akt is a downstream target of NF-κ B. J Biol Chem 2002;277:29674–80.
25. Schweitzer R, Shilo BZ. A thousand and one roles for the Drosophila EGF receptor. Trends Genet 1997;13:191–6.
26. Schilling B, De Medina T, Syken J, Vidal M, Munger K. A novel human DnaJ protein, hTid-1, a homolog of the Drosophila tumor suppressor protein Tid56, can interact with the human papillomavirus type 16 E7 oncoprotein. Virology 1998;247:74–85.
27. Edwards KM, Munger K. Depletion of physiological levels of the human TID1 protein renders cancer cell lines resistant to apoptosis mediated by multiple exogenous stimuli. Oncogene advance online publication 2004;1–13.